

# Experimental investigation of phase equilibria and thermodynamic modeling of the CaO-SiO<sub>2</sub>-Al<sub>2</sub>O<sub>3</sub>-CaS oxysulfide system

Rongxun Piao\*, Youn-Bae Kang, and Hae-Geon Lee

Graduate Institute of Ferrous Technology, Pohang University of Science and Technology, Pohang, Rep. of Korea

**Abstract:** Phase equilibria of the CaO-Al<sub>2</sub>O<sub>3</sub>-CaS, CaO-SiO<sub>2</sub>-CaS, and CaO-SiO<sub>2</sub>-Al<sub>2</sub>O<sub>3</sub>-CaS systems under low oxygen partial pressure have been experimentally investigated using equilibration and quenching techniques. Equilibrium phases were analyzed by Electron Probe X-ray Microanalysis (EPMA), and X-ray diffraction (XRD) analysis. Liquidus lines of all solid phases were successfully constructed in the temperature range investigated in the present study. In order to supplement the understanding of the phase equilibria, a thermodynamic modeling for this liquid oxysulfide were conducted using the Modified Quasichemical Model in the Quadruplet Approximation (MQMQA) assisted by the experimental data obtained in the present study as well as those available in literatures. A thermodynamic database for the CaO-SiO<sub>2</sub>-Al<sub>2</sub>O<sub>3</sub>-CaS system was developed in order to allow calculations of phase diagrams of various sections. This work is an extension of the previous thermodynamic modeling of sulfide capacity in the CaO-SiO<sub>2</sub>-Al<sub>2</sub>O<sub>3</sub> slag system, thereby forming a consistent set of database. Liquidus projections of those oxysulfide systems are proposed for the first time using the thermodynamic model and the database.

**Key words:** Phase Equilibria, CaO-Al<sub>2</sub>O<sub>3</sub>-SiO<sub>2</sub>-CaS system, Thermodynamics, Oxysulfide

## 1. Introduction

Ca injection into Al-killed steel is a common practice in secondary refining process in order to modify harmful solid alumina inclusions into liquid calcium aluminate (or calcium aluminosilicate) inclusions. This reduces the occurrence of nozzle clogging during the casting process and surface defects in the final product. However, depending on a S content in the molten steel, the Ca injected into the steel is also consumed by forming solid sulfide inclusion (CaS), some of which may dissolve into the liquid inclusion. Similar to the solid alumina, the solid CaS inclusions are also harmful to the castability of liquid steel. Thus, formation of the liquid inclusions is very important and desirable in order to reduce the nozzle clogging and the surface defect. Previously, most experimental investigations<sup>[1-11]</sup> on these systems have been focused on dilute concentration of sulfur in the oxide slags because attention was given to desulfurization of molten steel using top slag. A number of model equations also have been proposed to calculate sulfide capacity of multicomponent slags which can be directly applied for the slags with dilute concentration of sulfur.<sup>[12-17]</sup> On the other hand, the inclusions composed of CaO-SiO<sub>2</sub>-Al<sub>2</sub>O<sub>3</sub>-CaS may contain much higher sulfur concentration (a few percent of sulfur), thus those may be categorized as oxysulfide inclusion. As mentioned above, depending on the S concentration in the steels, inclusions may be solid sulfide or liquid oxysulfide or mixture of both phases. Therefore, in order to control inclusions evolution in the steels more effectively, phase equilibria and thermodynamics of the CaO-SiO<sub>2</sub>-Al<sub>2</sub>O<sub>3</sub>-CaS system should be clearly understood.

Previous experimental investigations on phase equilibria in the CaO-Al<sub>2</sub>O<sub>3</sub>-CaS<sup>[10,11,18-20]</sup>, CaO-SiO<sub>2</sub>-CaS<sup>[21-25]</sup> and

CaO-Al<sub>2</sub>O<sub>3</sub>-SiO<sub>2</sub>-CaS<sup>[26]</sup> systems were only focused on solubility of CaS, and inconsistencies were often observed, in particular for CaO-SiO<sub>2</sub>-CaS system. In the CaO-Al<sub>2</sub>O<sub>3</sub>-CaS system, the reported solubility of CaS in liquid oxysulfide decreases while concentration of CaO increases. On the other hand, there were discrepancies in the reported solubility of CaS in liquid oxysulfide of the CaO-SiO<sub>2</sub>-CaS system. Some investigations reported that solubility of CaS in liquid oxysulfide increases when concentration of CaO increases<sup>[23-25]</sup>, while there were opposite results showing decrease of the solubility of CaS.<sup>[21-22]</sup> There has not been further confirmation on this issue.

Thermodynamic modeling and subsequent calculations are proved to be very useful in prediction of phase equilibria (*i.e.*, solubility of CaS in liquid oxysulfide) and thermodynamic properties such as sulfide capacity in the liquid oxysulfide. For sulfide capacity calculations, there has been a number of model equations have been proposed.<sup>[12-17]</sup> Contrary to this, there has been very few models proposed for the calculation of phase equilibria including liquid oxysulfide.<sup>[14,17,27]</sup> Earlier proposal by Gaye and Lehmann<sup>[27]</sup> showed good agreement with the available CaS solubility data up to the time when their investigation was carried out. Unfortunately, the model (IRSID's model) has not been opened to public. The model has been further extended to cover whole oxysulfide composition by the same authors and have shown good agreement with phase diagram data in Mn-Si-O-S and Mn-Fe-O-S systems.<sup>[14]</sup> Recently, another model within the framework of the Modified Quasichemical Model in the Quadruplet Approximation (MQMQA)<sup>[28]</sup> has been developed by Kang and Pelton<sup>[17]</sup> and showed a good prediction for sulfide capacity of multicomponent molten oxide slags without any fitting parameters. In this model, the sulfide capacities are calculated from Gibbs energy of mixing of the oxysulfide liquid by considering various quadruplets as model components. Therefore, the model can also be applicable to the calculation of phase equilibria. Good agreement between model predictions and experimentally obtained phase diagram for MnO-SiO<sub>2</sub>-Al<sub>2</sub>O<sub>3</sub>-MnS system and its sub-system was shown.<sup>[17,29]</sup> The same model also has been applied for the calculation of a phase diagram section in the CaO-Al<sub>2</sub>O<sub>3</sub>-CaS system, but predicted somewhat higher CaS solubility in the liquid oxysulfide.<sup>[30]</sup> Most of the previous experimental investigations for the CaS solubility in CaO-Al<sub>2</sub>O<sub>3</sub>-SiO<sub>2</sub>-CaS system and its sub-systems<sup>[10,11,18-26]</sup> employed chemical equilibration of oxide samples under controlled O<sub>2</sub>/S<sub>2</sub> gas atmosphere, and X-ray diffraction (XRD) analysis was carried out for quenched samples in order to check whether solid CaS was saturated in the sample or not.

The purpose of the present study is (1) to measure phase equilibria of the CaO-SiO<sub>2</sub>-Al<sub>2</sub>O<sub>3</sub>-CaS system and its sub-systems not only for sulfide solubility but also for all other phase boundaries, (2) to give a general explanation of sulfur dissolution behavior in the high concentration range in the CaO-Al<sub>2</sub>O<sub>3</sub> and CaO-SiO<sub>2</sub> oxide systems, and (3) to refine the thermodynamic model of the oxysulfide CaO-SiO<sub>2</sub>-Al<sub>2</sub>O<sub>3</sub>-CaS system.

## 2. Experimental

The general procedure employed in the present study is that mixtures of oxide and sulfide powders were equilibrated at high temperatures and subsequently quenched in ice-brine. Chemical compositions of each phase in the quenched samples were determined by EPMA. The experimental apparatus employed in the present study is schematically shown in Figure 1.

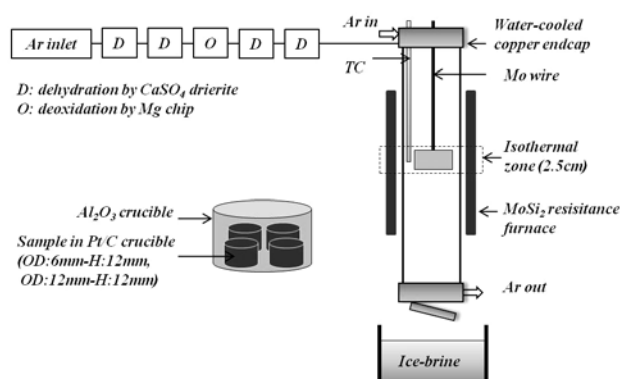


Figure 1. Schematic diagram of experimental apparatus employed in the present study.

Powder of CaO (99.9 mass%, supplied by Aldrich, USA), SiO<sub>2</sub> (99.9 mass%, supplied by Kojundo, Japan), Al<sub>2</sub>O<sub>3</sub> (99.9 mass%, supplied by Aldrich, USA) and CaS (99.99 mass%, supplied by Kojundo, Japan) were used as starting materials. Each mixture was weighed to 0.4 gram or 1 gram and placed in a Pt crucible (OD:6mm-H:12mm or OD:12mm-H:12mm) or carbon crucible (OD:12mm-H:12mm). Several crucibles containing in those mixtures were suspended by a molybdenum wire, which was surrounded by a recrystallized alumina reaction tube sealed by the water-cooled brass end-cap. The assembly was heated in a vertical resistance furnace with MoSi<sub>2</sub> heating elements under an atmosphere of Ar gas purified by passing through CaSO<sub>4</sub> column, and Mg chip at 450°C.

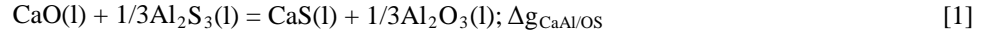
The temperature of the furnace was controlled by a thermocouple (Pt-6 pct Rh/Pt-30 pct Rh), which is connected to a proportional-integral-differential (PID) controller. In addition, the temperature of the samples was continuously monitored during the whole experiment by using another thermocouple, which is placed near the reaction crucible assembly. The temperature was controlled within  $\pm 1^\circ\text{C}$ .

The assembly was heated 0 - 50°C higher than a desired temperature for 1 hour and then, cooled to the desired temperature and equilibrated by keeping for 8 to 36 hours depending on sample compositions and temperature. Actual equilibration time for samples of two phases region such as liquid + CaS was confirmed through preliminary experiments by equilibrating the samples of the same composition with different holding times and it was confirmed that equilibration time for CaO-Al<sub>2</sub>O<sub>3</sub>-CaS system was about 5 hours and that for CaO-SiO<sub>2</sub>-CaS system was about 3 hour. Previous studies reported that 1 to 8 hours were chosen for equilibration time,<sup>[10,11,18-20,22]</sup> but in the present study, samples were equilibrated for longer time to ensure complete equilibrium over the whole composition range investigated in the present study.

### 3. Thermodynamic Calculation

In order to calculate phase equilibria of the systems concerned in the present study, thermodynamic optimizations and calculations were carried out. For the Gibbs energy of liquid oxysulfide, the Modified Quasichemical Model in the Quadruplet Approximation (MQMQA) developed by Kang and Pelton was employed.<sup>[17]</sup> In the model, it is assumed that the oxysulfide consists of two distinctive sublattices, for example, in the present system,  $(\text{Ca}^{2+}, \text{Si}^{4+}, \text{Al}^{3+})_x[\text{O}^{2-}$ ,

$S^{2-}]_y$ . Cations ( $Ca^{2+}$ ,  $Si^{4+}$ ,  $Al^{3+}$ ) reside exclusively on the cationic sublattice, whereas anions ( $O^{2-}$  and  $S^{2-}$ ) reside exclusively on anionic sublattice. Two important chemical reactions are considered in this model. One is the reciprocal reactions between pure liquid components in oxysulfide solution representing First-Nearest-Neighbor (FNN) short-range-ordering (SRO) such as shown in Eq. [1] and Eq. [2].



The other reaction that should be taken into account is the well-known strong Second-Nearest-Neighbor (SNN) SRO between cations over anions. For example, in the CaO-SiO<sub>2</sub> slag, the maximum SNN SRO occurs near Ca<sub>2</sub>SiO<sub>4</sub> composition where most Si<sup>4+</sup> cations have Ca<sup>2+</sup> cations in their second coordination shell. This is taken into account by the SNN pair exchange reaction such as shown in Eq. [3]



For the treatment of both FNN SRO and SNN SRO simultaneously, various quadruplet “clusters” that contain two cations and two anions such as CaCa/OO, CaSi/OO, CaAl/OS, AlAl/SS, *etc.*, are considered as basic entities of the model. There are total 18 different quadruplets in the present oxysulfide. These quadruplets are distributed randomly over “quadruplet” sites. A complete mathematical description of the model is given by Pelton *et al.*<sup>[28]</sup> The Gibbs energy of the solution is given by:

$$G = \sum_{\substack{i,j=Ca^{2+},Si^{4+},Al^{3+} \\ k,l=O^{2-},S^{2-}}} n_{ij/kl} g_{ij/kl} - T\Delta S^{config} \quad [4]$$

where  $n_{ij/kl}$  and  $g_{ij/kl}$  are the number of moles and the molar Gibbs energy of the “ $ij/kl$ ” quadruplets and  $\Delta S^{config}$  is the configurational entropy of mixing, which is given by randomly distributing the quadruplets over the sublattices. When S is not considered, the model exactly reduces to the Modified Quasichemical Model in the Pair Approximation (MQMPA), and all required model parameters without S for the liquid oxide phase were reported by Eriksson *et al.*<sup>[31]</sup> and Eriksson and Pelton.<sup>[32]</sup> Gibbs energies of solid oxide phases in the CaO-SiO<sub>2</sub>-Al<sub>2</sub>O<sub>3</sub> system can also be found in the same references.<sup>[31,32]</sup> In the previous reports on sulfide capacity of CaO-SiO<sub>2</sub>-Al<sub>2</sub>O<sub>3</sub> liquid oxide,<sup>[17]</sup> Gibbs energies of pure liquid CaS, SiS<sub>2</sub> and Al<sub>2</sub>S<sub>3</sub> were further required and details were given in the reference.<sup>[17]</sup> For the phase diagram calculation in the CaO-Al<sub>2</sub>O<sub>3</sub>-CaS system shown by Kang and Pelton,<sup>[30]</sup> Gibbs energy of solid CaS was required, and it was taken from JANAF thermochemical table.<sup>[33]</sup> As mentioned in Sec. 1, however, some discrepancies were observed in the previous report<sup>[30]</sup> as well as in the present study which will be shown in Sec. 4, small adjustments to the Gibbs energies of relevant phases are introduced. All the thermodynamic calculations performed in the present study were carried out using FactSage thermochemical software.<sup>[34]</sup>

## 4. Results and Discussion

### 4.1. CaO-Al<sub>2</sub>O<sub>3</sub>-CaS System

Shown in Figure 2 is an isothermal section of CaO-Al<sub>2</sub>O<sub>3</sub>-CaS system at 1550°C. Solid symbols shown in the

figure are measured liquidus points of several solid phases obtained in the present study, and open symbols are reported liquidus of CaS (solubility limit of CaS in the liquid oxysulfide composed of CaO-Al<sub>2</sub>O<sub>3</sub>-CaS) by Cameron *et al.*,<sup>[18]</sup> Takenouchi *et al.*<sup>[20]</sup> and Ozturk and Turkdogan.<sup>[19]</sup> The reported data of Takenouchi *et al.*<sup>[20]</sup> and Ozturk and Turkdogan<sup>[19]</sup> are in good agreement with each other and also with the data measured in the present study. Some of Cameron *et al.*'s data do not agree with others' data. General tendency of the solubility of CaS in the liquid phase is such that when concentration of CaO increases, then the solubility of CaS also increases. Similar tendency was also observed in the present study and in the literatures<sup>[10,11]</sup> at other temperatures than 1550°C. In the present study, liquidus of other solid phases (CaO or CaAl<sub>2</sub>O<sub>4</sub>) were also measured and shown in the figure, which were not measured in the previous investigations.

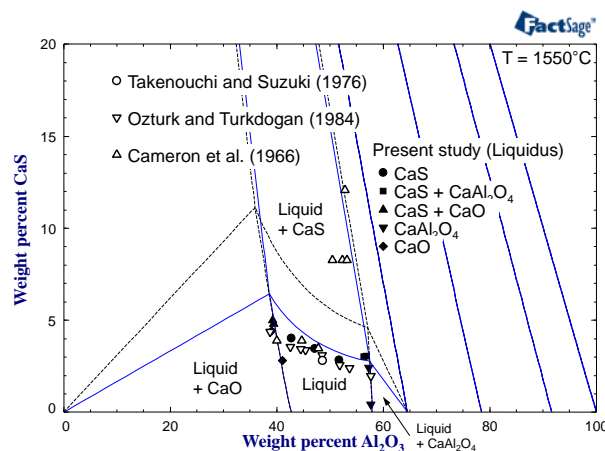


Figure 2. Isothermal section of CaO-Al<sub>2</sub>O<sub>3</sub>-CaS system at 1550°C. Symbols are experimental data. Full lines are calculated isothermal section in the present study, and dashed lines are calculated isothermal section before thermodynamic optimization.

Also shown in the Figure 2 are calculated isothermal section at 1550°C using thermodynamic model as described in Sec. 3. Dashed lines are calculated isothermal section using the thermodynamic model for the liquid oxysulfide phase as described in the previous articles<sup>[17,30]</sup> with no adjustment, thus it is solely predicted from the thermodynamic model with no fitting parameters. Although the dashed lines are sole prediction, the calculated liquidus of CaO and CaAl<sub>2</sub>O<sub>4</sub> are in good agreement with the experimental data obtained in the present study. However, the calculated solubility of CaS in the liquid phase is higher than the experimental data reported<sup>[18-20]</sup> as well as those in the present study. In the report of Kang and Pelton for the sulfide capacity in CaO-Al<sub>2</sub>O<sub>3</sub> slag,<sup>[17]</sup> the calculated sulfide capacity using the same model used for the calculation in the Figure 2 was in excellent agreement with the available experimental data in wide range of temperatures and compositions. Since the sulfide capacity is a thermodynamic property of the liquid phase only, this suggests that Gibbs energy of the liquid oxysulfide phase seems to be correct. Therefore, in order to improve the accuracy of the model calculation, the Gibbs energy of solid CaS phase has been adjusted from the value suggested in JANAF table.<sup>[33]</sup> After the adjustment of the Gibbs energy of solid CaS, calculated isothermal section shows better agreement with the experimental data as shown in the Figure 2 with solid lines. Similar conclusions could be also drawn at other temperatures. It is to be noted that the calculated solubility of CaS at 1550°C increases as

concentration of CaO increases, therefore it is in good accordance with the experimental data. Using the thermodynamic model, part of a liquidus projection of the CaO-Al<sub>2</sub>O<sub>3</sub>-CaS system at low S concentration has been calculated and is shown in Figure 3, showing general shape of liquidus of CaS in the system.

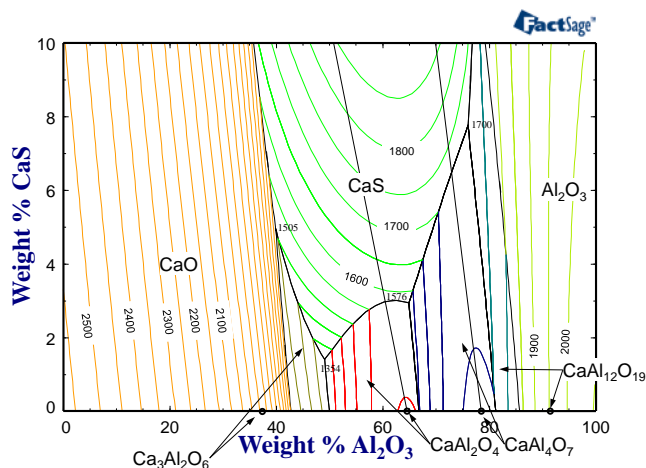


Figure 3. Calculated liquidus projection of the CaO-Al<sub>2</sub>O<sub>3</sub>-CaS system at low CaS concentration.

#### 4.2. CaO-SiO<sub>2</sub>-CaS System

Figure 4 shows an isothermal section of CaO-SiO<sub>2</sub>-CaS system at 1550°C. Solid symbols shown in the figure are measured liquidus points of several solid phases obtained in the present study, and open symbols are reported liquidus of CaS (solubility limit of CaS in the liquid oxysulfide composed of CaO-SiO<sub>2</sub>-CaS) by Sharma and Richardson.<sup>[21]</sup> The reported solubility data of Sharma and Richardson<sup>[21]</sup> are slightly higher than that of the present study. However, general tendency of the solubility of CaS in the liquid phase in both studies agree that when concentration of CaO increases, then the solubility of CaS decreases. This is an opposite trend to that observed in the CaO-Al<sub>2</sub>O<sub>3</sub>-CaS system. Measured solubility of CaS is generally higher than that in the CaO-Al<sub>2</sub>O<sub>3</sub>-CaS system at the same CaO concentration. Similar tendency was also observed in the present study and in the literatures<sup>[21,22]</sup> at other temperatures than 1550°C, while some investigations reported on opposite tendency.<sup>[23-25]</sup> In the present study, liquidus of other solid phases (Ca<sub>2</sub>SiO<sub>4</sub> or SiO<sub>2</sub>) were also measured and shown in the figure, which were not measured in the previous investigations.

Calculated isothermal section at 1550°C using thermodynamic model as described in Sec. 3 are also shown in the Figure 4. Dashed lines and solid lines have the same meaning as those shown in the Figure 2 that the dashed lines are calculated isothermal section using the thermodynamic model for the liquid oxysulfide phase as described in the previous reports by Kang and Pelton<sup>[17]</sup> with no adjustment even for the Gibbs energy of solid CaS, thus it is solely predicted from the thermodynamic model with no fitting parameters. Although the dashed lines shows favorably good agreement with the experimental data, the modification of the Gibbs energy of solid CaS as described in Sec. 4.1 would results in lowering solubility of CaS in the liquid oxysulfide phase. Therefore, it was necessary to introduce a small adjustable model parameter in the liquid CaO-SiO<sub>2</sub>-CaS oxysulfide phase in order to have good agreement with the

experimentally obtained CaS liquidus data even after the modification of Gibbs energy of the solid CaS. After the introduction of the small model parameter to the Gibbs energy of the liquid CaO-SiO<sub>2</sub>-CaS oxysulfide phase, calculated isothermal section shows an agreement with the experimental data as shown in the Figure 4 with solid lines. Similar conclusions could be also drawn at other temperatures. It is to be noted that the calculated solubility of CaS at 1550°C decreases as concentration of CaO increases. Introducing the model parameter would affect on the calculation of sulfide capacity in the CaO-SiO<sub>2</sub> slag shown in Kang and Pelton,<sup>[17]</sup> however, it was found that the difference caused by this additional model parameter was very small and was acceptable within uncertainties of sulfide capacity data. Using the thermodynamic model, part of a liquidus projection of the CaO-SiO<sub>2</sub>-CaS system at low S concentration has been calculated and is shown in Figure 5, showing general shape of liquidus of CaS in the system.

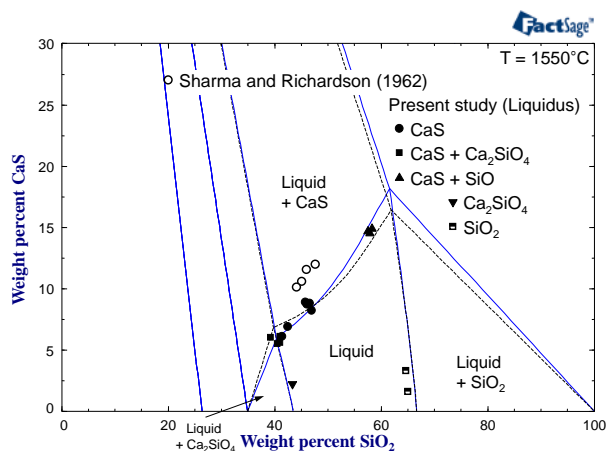


Figure 4. Isothermal section of CaO-SiO<sub>2</sub>-CaS system at 1550°C. Symbols are experimental data. Full lines are calculated isothermal section in the present study, and dashed lines are calculated isothermal section before thermodynamic optimization.

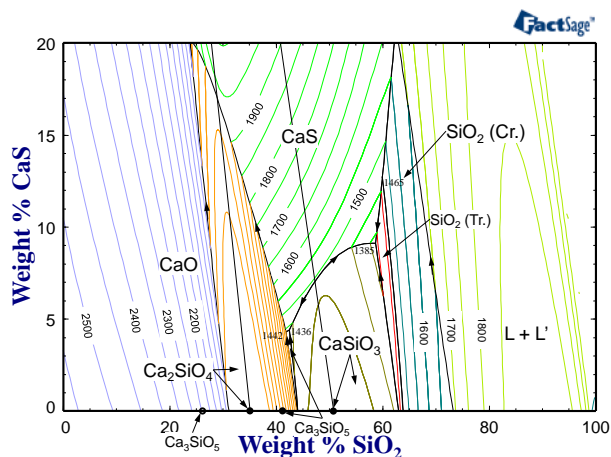


Figure 5. Calculated liquidus projection of the CaO-SiO<sub>2</sub>-CaS system at low CaS concentration.

### 4.3. CaO-Al<sub>2</sub>O<sub>3</sub>-SiO<sub>2</sub>-CaS System

Phase diagram investigation was further extended to the CaO-Al<sub>2</sub>O<sub>3</sub>-SiO<sub>2</sub>-CaS system at 1500°C. All the investigations were carried out at CaS saturation along with constant SiO<sub>2</sub> concentration in liquid oxysulfide phase in

order to represent the obtained data in 2-dimensional plane. Figures 6 and 7 show isothermal-isoplethal sections of the CaO-Al<sub>2</sub>O<sub>3</sub>-SiO<sub>2</sub>-CaS system at 1500°C at 4 wt% and 11 wt% SiO<sub>2</sub>, respectively. Symbols represent measured solubility of CaS in the liquid phase at the same condition although actual SiO<sub>2</sub> concentrations in the liquid phase vary from 4.0 to 4.5 wt % and 11.1 to 11.3 wt%, respectively. Since its low SiO<sub>2</sub> concentration, the solubility of CaS increases as CaO concentration increases, similar to the CaO-Al<sub>2</sub>O<sub>3</sub>-CaS system shown in Sec. 4.1. Increasing SiO<sub>2</sub> concentration also increases solubility of CaS at a given CaO/Al<sub>2</sub>O<sub>3</sub> ratio. Lines shown in the figures are calculated phase boundaries at 4 wt% SiO<sub>2</sub> and 11 wt% SiO<sub>2</sub> respectively, after the thermodynamic optimization carried out in the present study. Agreement between calculation and experimental data for the CaS solubility are favorably good.

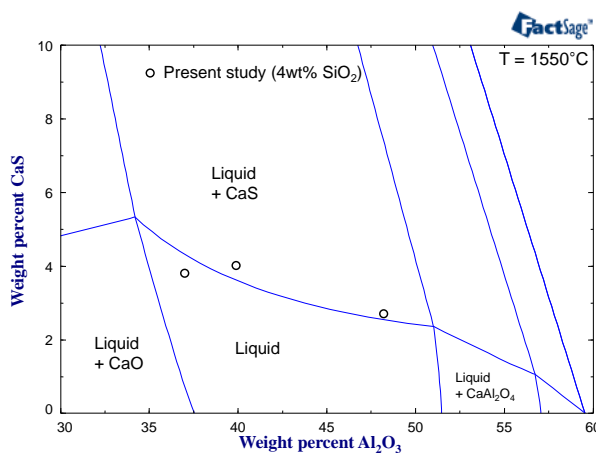


Figure 6. Isothermal-isoplethal section of CaO-Al<sub>2</sub>O<sub>3</sub>-SiO<sub>2</sub>-CaS system along 4wt% SiO<sub>2</sub> at 1500°C. Symbols are experimental data. Lines are calculated isothermal section in the present study.

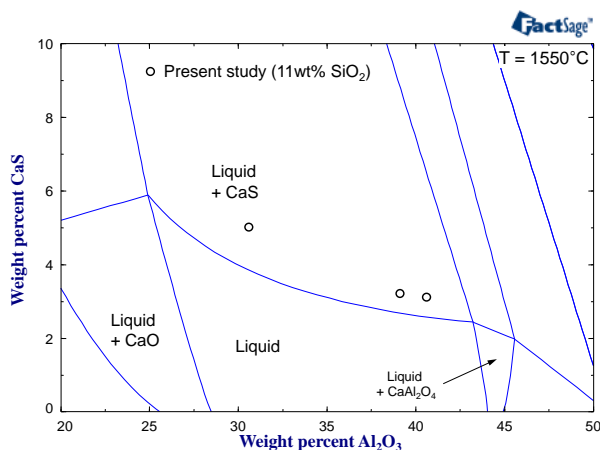


Figure 7. Isothermal-isoplethal section of CaO-Al<sub>2</sub>O<sub>3</sub>-SiO<sub>2</sub>-CaS system along 11wt% SiO<sub>2</sub> at 1500°C. Symbols are experimental data. Lines are calculated isothermal section in the present study.

#### 4.4. Behavior of CaS solubility in the CaO-Al<sub>2</sub>O<sub>3</sub>-CaS and CaO-SiO<sub>2</sub>-CaS Systems

As shown in Figures 2 and 4, solubility of the CaS in the liquid oxysulfide depends on composition of CaO in the liquid phase, but trend of such dependence is different between the CaO-Al<sub>2</sub>O<sub>3</sub>-CaS system and the CaO-SiO<sub>2</sub>-CaS

system. Increasing CaO concentration in the liquid CaO-Al<sub>2</sub>O<sub>3</sub>-CaS oxysulfide phase increases the solubility of CaS, while increasing CaO concentration in the liquid CaO-SiO<sub>2</sub>-CaS oxysulfide phase decreases the solubility of CaS. No clear explanation on such phenomena has been found in literatures. Such phenomena appear to be related to competitive interactions between cation – anion as FNN interaction and cation – cation as SNN interaction. First, let us consider the solubility of CaS in the CaO-Al<sub>2</sub>O<sub>3</sub>-CaS system as shown in Figure 2. The reciprocal reaction [1] may be taken into account, and the associated Gibbs energy for the reaction is ~ 172kJ/mol at 1550°C which is very negative.<sup>[17]</sup> Therefore, most Ca and S will attract each other and Al and O will attract each other, compared to a hypothetical ideal mixture (*i.e.*,  $\Delta g_{CaAl/Os} = 0$ ). This corresponds to the FNN SRO as mentioned in Sec. 3. It results in a positive deviation between the CaS and Al<sub>2</sub>O<sub>3</sub> compared to the ideal mixture, therefore activity coefficient of CaS increases as concentration of Al<sub>2</sub>O<sub>3</sub> increases. Since activity of the CaS in the liquid oxysulfide at the solubility limit of CaS is always unity, consequently, concentration of CaS should decrease as concentration of Al<sub>2</sub>O<sub>3</sub> increases. This is consistent with the observation in the CaO-Al<sub>2</sub>O<sub>3</sub>-CaS system as shown in Figure 2. A similar consideration was given to MnO-SiO<sub>2</sub>-Al<sub>2</sub>O<sub>3</sub>-MnS system by Kim *et al.* for the solubility of MnS in the liquid MnO-SiO<sub>2</sub>-Al<sub>2</sub>O<sub>3</sub>-MnS oxysulfide phase.<sup>[29]</sup>

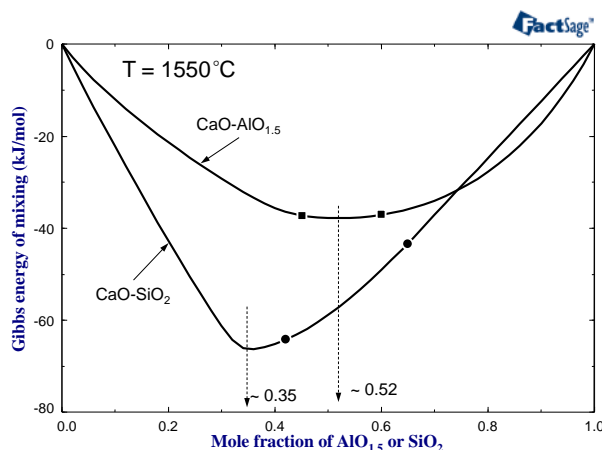


Figure 8. Calculated Gibbs energies of mixing of liquid CaO-AlO<sub>1.5</sub> and CaO-SiO<sub>2</sub> oxides at 1550°C. Symbols represent homogeneous liquid phase boundaries at 1550° in each system.

On the other hand, such FNN SRO alone is not sufficient to account for the solubility of CaS observed in the CaO-SiO<sub>2</sub>-CaS system shown in Figure 4. This seems to be attributed to the fact that there is a very strong attraction between Ca and Si cations over oxygen anion as a SNN SRO. Shown in Figure 8 is the calculated Gibbs energy of mixing of CaO-AlO<sub>1.5</sub> (half of Al<sub>2</sub>O<sub>3</sub>) and CaO-SiO<sub>2</sub> slags at 1550°C.<sup>[31,32]</sup> Stable liquid phases are only observed between compositions marked by symbols in each system. The Gibbs energy of mixing of CaO-SiO<sub>2</sub> liquid is much negative, and shows a sharp minimum at  $X_{SiO_2} = \sim 0.35$ , representing strong SNN SRO maximized at this composition. On the other hand, that of CaO-AlO<sub>1.5</sub> liquid is less negative than that of the CaO-SiO<sub>2</sub> liquid, and does not show such sharp minimum, suggesting less pronounced SNN SRO. Such SNN SRO in the oxide liquids affects on the Gibbs energy of mixing in oxysulfide and the resultant Gibbs energies of mixing in two liquid oxisulfides, CaO-Al<sub>2</sub>O<sub>3</sub>-CaS and CaO-SiO<sub>2</sub>-CaS, are calculated from the thermodynamic model which takes into account both FNN SRO and SNN

SRO, and are shown in Figures 9 and 10, respectively. The Gibbs energy of mixing is represented with respect to pure liquid CaO,  $\text{AlO}_{1.5}$  (or  $\text{SiO}_2$ ) and CaS, along constant  $n_{\text{AlO}_{1.5}} / (n_{\text{CaO}} + n_{\text{AlO}_{1.5}})$  (or  $n_{\text{SiO}_2} / (n_{\text{CaO}} + n_{\text{SiO}_2})$ ). In Figure 9, the Gibbs energy of mixing of the liquid CaO- $\text{AlO}_{1.5}$ -CaS oxysulfide is shown. Solubility of CaS in the liquid phase can be obtained by taking a tangent of the Gibbs energy of mixing to Gibbs energy of solid CaS (marked as open circle). Since there is no strong SNN SRO in the liquid CaO- $\text{AlO}_{1.5}$  oxide phase, the obtained solubility of CaS (marked as solid symbols) increases as concentration of CaO increases. This is consistent with what experimentally was observed. On the other hand, according to the Gibbs energy of mixing of the liquid CaO- $\text{SiO}_2$ -CaS oxysulfide shown in the Figure 10, due to strong SNN SRO in liquid CaO- $\text{SiO}_2$  oxide phase, the Gibbs energy of mixing is shifted downward and the shift becomes most evident near the composition of maximum SNN SRO ( $X_{\text{SiO}_2} = \sim 0.35$ ). Therefore, between 0.4 to 0.6 in terms of  $n_{\text{SiO}_2} / (n_{\text{CaO}} + n_{\text{SiO}_2})$  where liquid phase is stable (see Figure 8), increasing concentration of CaO decreases the solubility of CaS in the liquid CaO- $\text{SiO}_2$ -CaS oxysulfide (marked as solid symbols). This is now consistent with experimental data.

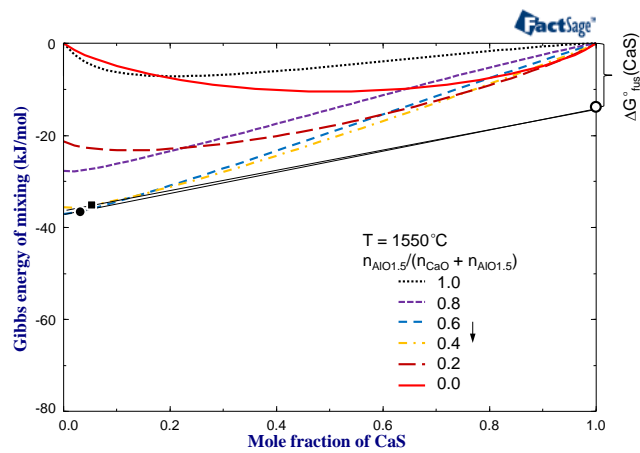


Figure 9. Calculated Gibbs energies of mixing of liquid CaO- $\text{AlO}_{1.5}$ -CaS oxysulfide at 1550°C along iso- $n_{\text{AlO}_{1.5}}/(n_{\text{CaO}} + n_{\text{AlO}_{1.5}})$ . Open circle represents the Gibbs energy of fusion of CaS and solid symbols represent solubility limit of CaS in the liquid oxysulfide at each  $n_{\text{AlO}_{1.5}}/(n_{\text{CaO}} + n_{\text{AlO}_{1.5}})$ .

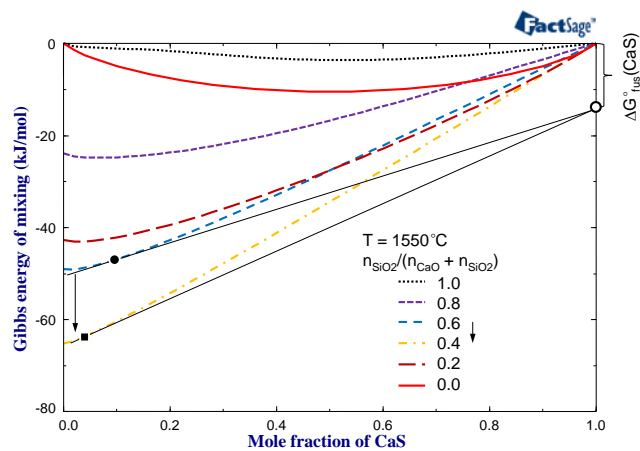


Figure 10. Calculated Gibbs energies of mixing of liquid CaO- $\text{SiO}_2$ -CaS oxysulfide at 1550°C along iso- $n_{\text{SiO}_2}/(n_{\text{CaO}} + n_{\text{SiO}_2})$ . Open circle represents the Gibbs energy of fusion of CaS and solid symbols represent solubility limit of CaS in the liquid oxysulfide at each  $n_{\text{SiO}_2}/(n_{\text{CaO}} + n_{\text{SiO}_2})$ .

of CaS in the liquid oxysulfide at each  $n_{\text{AlO}_{1.5}}/(n_{\text{CaO}} + n_{\text{AlO}_{1.5}})$ .

In short, in order to describe thermodynamic behavior of liquid oxysulfide and to calculate phase equilibria involving the liquid oxysulfide, both FNN SRO and SNN SRO should be taken into account. As described in Sec. 3, the thermodynamic calculations carried out in the present study take into account both in the framework of MQMQA. As a result, the phase equilibria measured in the present study as well as those available in literatures are well accounted for by the present approach.

## 5. Conclusion

Phase equilibria of CaO-Al<sub>2</sub>O<sub>3</sub>-CaS, CaO-SiO<sub>2</sub>-CaS, and CaO-SiO<sub>2</sub>-Al<sub>2</sub>O<sub>3</sub>-CaS system were experimentally measured by employing equilibrium/quenching technique. Thermodynamic modeling of the CaO-SiO<sub>2</sub>-Al<sub>2</sub>O<sub>3</sub>-CaS oxysulfide system has been conducted by using Modified Quasichemical Model in the Quadruplet Approximation.<sup>[17,28]</sup> Thermodynamic database for the CaO-SiO<sub>2</sub>-Al<sub>2</sub>O<sub>3</sub>-CaS system was optimized to allow calculation of phase diagrams based on the experimental data obtained in the present study as well as those available in literatures. Liquidus projections of the CaO-SiO<sub>2</sub>-CaS and CaO-Al<sub>2</sub>O<sub>3</sub>-CaS ternary systems were proposed for the first time using the thermodynamic model and the database. A general interpretation for the dissolution behavior of sulfur in the high concentration range in the liquid solution was proposed by considering the FNN- and SNN- SRO. In the CaO-Al<sub>2</sub>O<sub>3</sub>-CaS system, experimentally measured solubility of calcium sulfide showed an increasing tendency as increasing CaO concentration and this is because the interaction from FNN exchange reaction governs the dissolution of calcium sulfide than the interaction between the SNN pairs. In the case of CaO-SiO<sub>2</sub>-CaS system, however, solubility of CaS shows decreasing tendency and this is attributed to the fact that the contribution from the SNN SRO is considerable in this highly ordered system.

## Acknowledgement

This work was financially supported by POSCO Ltd. through Steel Innovation Program to Graduate Institute of Ferrous Technology, Pohang University of Science and Technology.

## References

- [1] C.J.B. Fincham and F.D. Richardson. The Behavior of Sulphur in Silicate and Aluminate Melts. Proc. Roy. Soc., 1954, 223A, p 40-62.
- [2] K.P. Abraham, M.W. Davies and F.D. Richardson. Sulfide Capacities of Silicate Melts. I. J. Iron and Steel Inst., 1960, 196, p 309-312.
- [3] P.T. Carter and T.G. Macfarlane. Thermodynamics of Slag Systems. J. Iron and Steel Inst., 1957, 185, p 54-66.
- [4] S.D. Brown, R.J. Roxburgh, I. Ghita and H.B. Bell. Sulphide Capacity of Titania-Containing slags. Ironmaking and Steelmaking, 1982, 9, p 163-167.
- [5] M. Gernerup and O. Wijk. Sulfide Capacities of CaO-Al<sub>2</sub>O<sub>3</sub>-SiO<sub>2</sub> Slags at 1550, 1600 and 1650°C. Scand. J. Metall., 1996, 25, p 103-107.

- [6] M. Chapman, O. Ostrovski, G. Tranell and S. Jahanshahi. Sulfide Capacity of Titania-Containing Slags. *Elektrometallurgiya*, 2000, p 34-39.
- [7] K.P. Abraham and F.D. Richardson. Sulfide Capacities of Silicate Melts. II. *J. Iron and Steel Inst.*, 1960, 196, p 313-317.
- [8] E. Drakaliysky, D. Sichen and S. Seetharaman. An Experimental Study of the Sulphide Capacities in the System  $\text{Al}_2\text{O}_3\text{-CaO-SiO}_2$ . *Can. Metall. Quart.*, 1997, 36, p 115-120.
- [9] M. Hino, S. Kitagawa and S. Ban-Ya. Sulphide Capacities of  $\text{CaO-Al}_2\text{O}_3\text{-MgO}$  and  $\text{CaO-Al}_2\text{O}_3\text{-SiO}_2$  Slags. *ISIJ Int.*, 1993, 33, p 36-42.
- [10] G.J.W. Kor and F.D. Richardson. Sulphur in Lime-Alumina Mixtures. *J. Iron and Steel Inst.*, 1968, 206, p 700-704.
- [11] R.A. Sharma and F.D. Richardson. Activities in Lime-Alumina Melts. *J. Iron and Steel Inst.*, 1961, 198, p 386-390.
- [12] D.J. Sosinsky and I.D. Sommerville, The Composition and Temperature Dependence of the Sulfide Capacity of Metallurgical Slags. *Metall. Trans. B.*, 1986, 17B, p 331-337.
- [13] M.M. Nzotta, M. Andreasson, P. Jönsson and S. Seetharaman. A study on the Sulfide Capacities of Steelmaking Slags. *Scand. J. Metall.*, 2000, 29, p 177-184.
- [14] H. Gaye and J. Lehmann. Modelling of Slag Thermodynamic Properties. From Oxides to Oxisulphides. *Proc. 5th Int'l. Conference on Molten Slags, Fluxes and Salts, ISS, Warrendale, PA, 1997*, pp. 27-34.
- [15] R.G. Reddy and M. Blander. Modeling of Sulfide Capacities of Silicate Melts. *Metall. Trans. B.*, 1987, 18B, p 591-569.
- [16] A.D. Pelton, G. Eriksson and A. Remero-Serrano. Calculation of Sulfide Capacities of Multicomponent Slags. *Metall. Trans. B.*, 1993, 24B, p 817-825.
- [17] Y.-B. Kang and A.D. Pelton. Thermodynamic Model and Database for Sulfides Dissolved in Molten Oxide Slags *Metall. Trans. B.*, 2009, 40B, p 979-994.
- [18] J. Carmeron, T.B Gibbons, and J. Taylor. Calcium Sulphide Solubilities and Lime Activities in the Lime-Alumina-Silica System. *J. Iron and Steel Inst.*, 1966, p 1223-1228.
- [19] B. Ozturk and E.T. Turkdogan. Equilibrium S Distribution Between Molten Calcium Aluminate and Steel Part 1  $\text{CaS-CaO-Al}_2\text{O}_3$  Melts Equilibrated with Liquid Fe Containing Al and S. *Metal Science*, 1984, 18, p 299-305.
- [20] T. Takenouchi and K. Suzuki. Influence of Ca-Al Deoxidizer on the Morphology of Inclusions. *Tetsu-to-Hagane*, 1976, 62, p 1653-1662.
- [21] R.A. Sharma and F.D. Richardson. The Solubility of Calcium Sulphide and Activities in Lime-Silica Melts. *J. Iron and Steel Inst.*, 1962, p 373-379.
- [22] K. Sawamura and M. Imaizumi. Solubility of Sulphur in  $\text{CaO-SiO}_2$  Binary Slags. *Tetsu-to-Hagane*, 1963, 49, p 1334-1336.
- [23] T. El Gammal and H.W. Hoehle. Determination of the Sulfur Activity in Lime-Silica slags at 1560°. *Archiv. Eisenhuettenwes.* 1970, 6, p 523-528.
- [24] R.S. McCaffery and J.F. Osterle. Desulfurizing Power of Iron Blast-Furnace Slags. *Trans. AIME*, 1923, 63, p 606-634.
- [25] A.S. Panov, I.S. Kulikov and L.M. Cylev. The Physicochemical Properties of Sulfide-Silicate Melts.

Fiziko-chimiceskie osnovy proidzvodstva stali Moskva.1964, p 100-106.

- [26] M. Uo, E. Sakurai, F. Tsukihashi, and N. Sano. The CaS Solubility in the CaO Bearing Slags. *Steel research*, 1989, 11, p 496-502.
- [27] H. Gaye and J. Lehmann. Sulphide Capacities. *Slag Atlas*, 2nd Edition, Verlag Stahleisen GmbH, 1995, p 266
- [28] A.D. Pelton, P. Chartrand and G. Eriksson. The Modified Quasichemical Model: Part IV. Two-Sublattice Quadruplet Approximation. *Metall. Mater. A*, 2001, 32A, p 1409-1416.
- [29] Y.-J. Kim, D.-H. Woo, H. Gaye, H.-G. Lee and Y.-B. Kang. Thermodynamics of MnO-SiO<sub>2</sub>-Al<sub>2</sub>O<sub>3</sub>-MnS Liquid Oxysulfide: Experimental and Thermodynamic Modeling. *Metall. Mater. B*, 2011, 42B, p 535-545.
- [30] Y.-B. Kang and A.D. Pelton. Thermodynamic Databases and Their Applications for Sulfur Control in Steelmaking. *Proc. of Asia Steel 2009*, 2009, p S3-42.
- [31] G. Eriksson, P. Wu, M. Blander and A.D. Pelton. Critical Evaluation and Optimization of the Thermodynamic Properties and Phase Diagrams of the MnO-SiO<sub>2</sub> and CaO-SiO<sub>2</sub> Systems. *Canad. Met. Quart.*, 1994, 33, p 13-22.
- [32] G. Eriksson and A.D. Pelton. Critical Evaluation and Optimization of the Thermodynamic Properties and Phase Diagrams of the CaO-Al<sub>2</sub>O<sub>3</sub>, Al<sub>2</sub>O<sub>3</sub>-SiO<sub>2</sub>, and CaO-Al<sub>2</sub>O<sub>3</sub>-SiO<sub>2</sub> Systems. *Metall. Trans. B*, 1993, 24B, p 807-816.
- [33] D.R. Stull and H. Prophet. *JANAF Thermochemical Tables*, U.S. Department of Commerce, Washington, DC, 1985.
- [34] C.W. Bale, E. Bélisle, P. Chartrand, S.A. Decterov, G. Eriksson, K. Hack, I.-H. Jung, Y.-B. Kang, J. Melançon, A.D. Pelton, C. Robelin, S. Petersen. *FactSage Thermochemical Software and Databases - Recent Developments*. *Calphad*, 2009, 33, p 295-311.